

# Fast and Robust Tessellation-Based Silhouette Shadows

Tomáš Milet  
Brno University of  
Technology Czech  
Republic  
imilet@fit.vutbr.cz

Jozef Kobrtek  
Brno University of  
Technology Czech  
Republic  
ikobrtek@fit.vutbr.cz

Pavel Zemčík  
Brno University of  
Technology Czech  
Republic  
zemcik@fit.vutbr.cz

Jan Pečiva  
Brno University of  
Technology Czech  
Republic  
peciva@fit.vutbr.cz

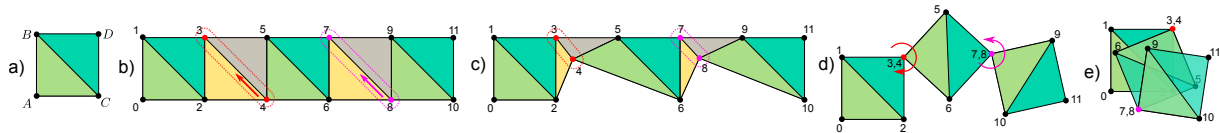


Figure 1: The image shows the transformation of a quad into three overlapping shadow volume sides. The transition from part a) to part b) is tessellation of quad with Multiplicity = 3. Only green and blue triangles will be drawn. Yellow and gray triangles will be degenerated. The transition from part b) over part c) to part d) shows degeneration process. Red and purple vertices 3, 4 and 7, 8 from part a) form only one vertex in part d). The transition from part d) to part e) shows rotation around red and purple vertices. This transformation creates three overlapping sides of shadow volume. Positions of vertices A, B, C, D that form initial quad, can be computed according to equations 2.

## ABSTRACT

This paper presents a new simple, fast and robust approach in computation of per-sample precise shadows. The method uses tessellation shaders for computation of silhouettes on arbitrary triangle soup. We were able to reach robustness by our previously published algorithm using deterministic shadow volume computation. We also propose a new simplification of the silhouette computation by introducing reference edge testing. Our new method was compared with other methods and evaluated on multiple hardware platforms and different scenes, providing better performance than current state-of-the-art algorithms. Finally, conclusions are drawn and the future work is outlined.

**Keywords:** shadows, shadow volumes, silhouette, tessellation shaders, geometry shader

## 1 INTRODUCTION

Shadow Volumes (SV) algorithm was introduced in 1977 by [Crow, 1977], first implementation using hardware support via stencil buffer was carried out by [Heidmann, 1991]. Heidman's implementation is generally called z-pass, but does not produce correct results when observer is in shadow. This problem was eliminated in the z-fail method [Everitt and Kilgard, 2002], which reverses depth test function, but requires shadow volumes to be capped.

Shadow Mapping (SM) algorithm, proposed by [Williams, 1978], is an alternative approach to shadow volumes. It uses depth information from light source stored in a texture. Shadow mapping is nowadays massively used in games thanks to its performance,

but suffers from spatial and often temporal aliasing problems and produces imperfect shadows because of limited shadow map resolution [Donnelly and Lauritzen, 2006]. Low resolution is not an issue for games, because scenes can be adjusted so that visual artifacts are suppressed or a filtering method is applied, but applications for visualization in architecture or industrial design require pixel-correct shadows for object visualization. Per-sample precise alias-free shadow maps (AFSM) algorithm was proposed by [Sintorn et al., 2008]. Their method stores multiple samples into a list for each shadow map pixel and conservatively rasterizes triangles into shadow map using CUDA. Individual samples stored in lists are then tested against shadow volume of the triangle. As they stated, their per-sample precise method is three times slower than standard shadow mapping with resolution of 8096 by 8096 texels.

While producing per-sample correct shadows, SV are affected by performance issues. In its naive form, when a volume is generated for every triangle in the scene, resulting performance is very low due to rasterization of a large amount of triangles. More efficient way is to construct shadow volumes only from silhouette edges

Permission to make digital or hard copies of all or part of this work for personal or classroom use is granted without fee provided that copies are not made or distributed for profit or commercial advantage and that copies bear this notice and the full citation on the first page. To copy otherwise, or republish, to post on servers or to redistribute to lists, requires prior specific permission and/or a fee.

of the occluding geometry, which has positive impact on fill-rate. Silhouette extraction on CPU was first published by [Brabec and Seidel, 2003].

Several silhouette-based methods were published since then, utilising novel hardware features to speed up silhouette calculation. [McGuire et al., 2003] managed to implement the algorithm in vertex shader and [Stich et al., 2007] used geometry shaders.

Most of the methods mentioned above are not completely robust and also cannot handle non 2-manifold casters. [Kim et al., 2008] proposed an algorithm for non 2-manifold casters, but unfortunately it is not robust. Kim’s algorithm was improved in [Pečiva et al., 2013] using deterministic multiplicity calculation, which we further simplified in this paper.

[Sintorn et al., 2011] also proposed a shadowing technique based on CUDA software rasterization of per-triangle shadow frusta. This technique uses a small bias when testing sample depth against a triangle plane to avoid self-shadowing. This bias, however, may cause a shadowed fragment to be lit in the final result, moreover, it is also scene-dependent.

## 2 METHOD DESCRIPTION

We have developed three methods - two per-triangle approaches and robust silhouette method.

Our silhouette method is based on the work of [Kim et al., 2008]. This algorithm calculates so-called *multiplicity* of an edge - light plane from light source through the edge is casted and all opposing vertices are tested, if they are above or below the plane. According to result of the test, multiplicity is incremented or decremented. Absolute value of multiplicity is the number of times an infinite quad needs to be drawn from this edge.

### 2.1 Per-Triangle Methods

These methods require no pre-processing and work with arbitrary triangle soup. In the first variant, input patch has 3 points, which are original points of the triangle. Tessellation factors are 3 (inner) and 1 (outer, for all sides), equal spacing and reversed triangle winding. The resulting patch can be seen in the picture 2b.

We construct a simple volume in evaluation shader as in Algorithm 1. Front cap needs to be rendered in second pass in order to close the volume.

We also designed a single-pass version for z-fail. This method takes a triangle as an input, but adds one more point to form a quad (4 control shader invocations per patch). This quad is then tessellated using outer factors (1, 5, 1, 5), inner (5,1) and fractional odd spacing, resulting in a shape seen in Fig. 3b.

Evaluation shader then twists the shape in order to create a volume, note Figure 3.

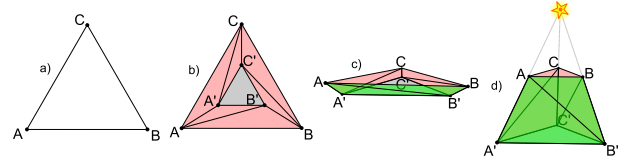


Figure 2: Creating semi-enclosed shadow volume from a triangle. Initial triangle in a) is tessellated using outer factors (1, 1, 1) and inner (3) b). Points  $A'$ ,  $B'$ ,  $C'$  are given positions of points  $A$ ,  $B$ ,  $C$  c) and then pushed to infinity to form a volume with back cap d).

**Data:** original points  $\mathbf{P}[3]$ , light position  $\mathbf{L}$ , tessellation coordinates  $\mathbf{T} = (x, y, z), x, y, z \in \langle 0, 1 \rangle$

**Result:** world-space coordinates  $X$

$c = x \cdot y \cdot z;$

**if**  $c == 0$  **then**

$\mathbf{X} = \mathbf{P}[0] \cdot x + \mathbf{P}[1] \cdot y + \mathbf{P}[2] \cdot z;$

$\mathbf{X}_w = 1;$

**else**

$i = \text{getIndexOfLargestVectorElement}(\mathbf{T});$

$\mathbf{X} = l_w \cdot \mathbf{P}[i] - \mathbf{L};$

$\mathbf{X}_w = 0;$

**end**

**Algorithm 1:** Evaluation shader in two-pass per-triangle method

### 2.2 Silhouette Method

The method finds silhouette edges by looping over every edge in the model. Each edge is processed in parallel in Tessellation Control Shader where multiplicity is computed. An input patch primitive is composed of two vertices that describe an edge, one integer that contains number of opposite vertices and  $n$  opposite vertices, see Figure 4. Because patch the size must be constant, some positions are not used.

A vertex buffer of model has to be extended by  $E_n$  vertices, which is the number of edges in the model. We used element buffer to reduce memory requirements.

Byungmoon’s algorithm [Kim et al., 2008], as in its core proposal, has a flaw that multiplicity is not calculated in a deterministic way. In older approach [Pečiva et al., 2013], it was fixed by calculating multiplicity per triangle and if the 3 results throughout all 3 edges were not consistent, we discarded the triangle from further processing, because it meant that the triangle is almost parallel to the light and does not cast a shadow. We further improved this approach - multiplicity is now computed only once for each opposite vertex using *reference edge*.

A choice of reference edge has to be the same for all occurrences of a triangle. This can be achieved for ex-

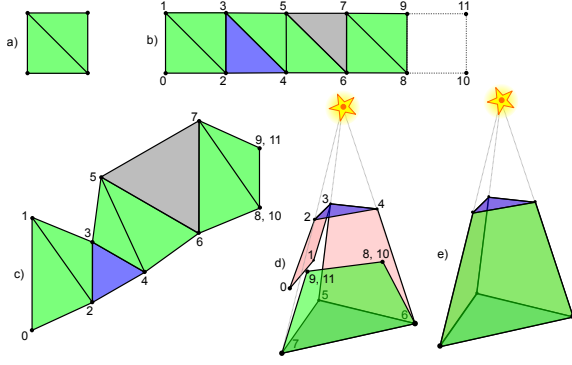


Figure 3: Single-pass per triangle method, a full shadow volume is created in a single pass. One point is added to the triangle in order to form a quad *a*) which is then tessellated using factors (1, 5, 1, 5), (5, 1) *b*). Points 10 and 11 are merged with 8, 9. Light cap is visualized as blue, dark cap grey *c*). Then we join points 0-7, 1-5, 2-9, 4-8 and push points 5, 6, 7 to infinity *d*) to make the volume *e*).

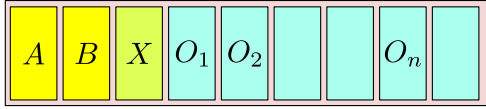


Figure 4: Input patch for tessellation control shader

ample by introducing vertex ordering - Equations 1 and Algorithm 2.

$$\begin{aligned}
 \mathbf{A} < \mathbf{B} &\Leftrightarrow \text{Greater}(\mathbf{A}, \mathbf{B}) < 0 \\
 \mathbf{A} = \mathbf{B} &\Leftrightarrow \text{Greater}(\mathbf{A}, \mathbf{B}) = 0 \\
 \mathbf{A} > \mathbf{B} &\Leftrightarrow \text{Greater}(\mathbf{A}, \mathbf{B}) > 0
 \end{aligned} \quad (1)$$

**Data:** Vertices  $\mathbf{A}, \mathbf{B}$

**Result:** Result  $r$  of comparison

$$\mathbf{S} = \text{sgn}(\mathbf{A} - \mathbf{B});$$

$$\mathbf{K} = (4, 2, 1);$$

$$r = \mathbf{S} \cdot \mathbf{K}$$

**Algorithm 2:** Function  $\text{Greater}(\mathbf{A}, \mathbf{B})$  used for vertex ordering.

In order to guarantee consistency, reference edge of a triangle in our algorithm is constructed using smallest and largest vertex of a triangle, as in Algorithm 2. More options for such method are available, but evaluation per each triangle occurrence must be consistent in order to get correct results.

To simulate behaviour of Byungmoon's algorithm (edge casts a quad as many times as it has multiplicity), we tessellate the casted quad from the edge using inner tessellation levels ( $\text{Multiplicity} \cdot 2 - 1, 1$ ) and then we bend the tessellated quad in evaluation shader in a way to create  $m$  overlapping quads, as seen in Fig. 1, which demonstrates edge  $\mathbf{A}-\mathbf{B}$  having multiplicity of 3.

The procedure of multiplicity calculation is described in Algorithm 3 and 4.

**Data:** Edge  $\mathbf{A}, \mathbf{B}, \mathbf{A} < \mathbf{B}$ , set  $\mathcal{O}$  of opposite vertices  $\mathbf{O}_i \in \mathcal{O}$ , light position  $\mathbf{L}$  in homogeneous coordinates

**Result:** Multiplicity  $m$

$$m = 0;$$

**for**  $\mathbf{O}_i \in \mathcal{O}$  **do**

**if**  $\mathbf{A} > \mathbf{O}_i$  **then**

$$m = m + \text{CompMultiplicity}(\mathbf{O}_i, \mathbf{A}, \mathbf{B}, \mathbf{L});$$

**else**

**if**  $\mathbf{B} > \mathbf{O}_i$  **then**

$$m = m - \text{CompMultiplicity}(\mathbf{A}, \mathbf{O}_i, \mathbf{B}, \mathbf{L});$$

**else**

$$m = m + \text{CompMultiplicity}(\mathbf{A}, \mathbf{B}, \mathbf{O}_i, \mathbf{L});$$

**end**

**end**

**end**

**Algorithm 3:** Modified algorithm for computation of final multiplicity of edge  $\mathbf{A}, \mathbf{B}$

**Data:** Vertices  $\mathbf{A}, \mathbf{B}, \mathbf{C}; \mathbf{A} < \mathbf{B} < \mathbf{C}$ ; light position  $\mathbf{L}$  in homogeneous coordinates

**Result:** Multiplicity  $m$  for one opposite vertex

$$\mathbf{X} = \mathbf{C} - \mathbf{A};$$

$$\mathbf{Y} = (l_x - a_x l_w, l_y - a_y l_w, l_z - a_z l_w);$$

$$\mathbf{N} = \mathbf{X} \times \mathbf{Y};$$

$$m = \text{sgn}(\mathbf{N} \cdot (\mathbf{B} - \mathbf{A}));$$

**Algorithm 4:**  $\text{CompMultiplicity}(\mathbf{A}, \mathbf{B}, \mathbf{C}, \mathbf{L})$  function used in algorithm 3

After tessellation, we have to transform tessellation coordinates into vertex position of the shadow volume in the evaluation shader. The algorithm for its implementation is described in Algorithm 5 and Equations 2.

$$\mathbf{A} = (a_x, a_y, a_z, 1)^T$$

$$\mathbf{B} = (b_x, b_y, b_z, 1)^T$$

$$\mathbf{C} = (a_x - l_x, a_y - l_y, a_z - l_z, 0)^T$$

$$\mathbf{D} = (b_x - l_x, b_y - l_y, b_z - l_z, 0)^T \quad (2)$$

Because caps are not generated, this method can also be used with simpler z-pass algorithm.

### 2.3 Implementation

All our methods were implemented in Lexolights, an open-source multi-platform program based on OpenSceneGraph and Delta3D, using OpenGL.

Single-pass per-triangle method suffers from inconsistent rasterization of two identical triangles at the same depth but with different winding - depth of fragments from both triangles differs, which resulted in z-fighting artifacts. We had to manually push the front cap's

**Data:** Vertices **A, B, C, D**, tessellation coordinates  $x, y \in \langle 0, 1 \rangle$  and multiplicity  $m$

**Result:** Vertex **V** in world-space

$\mathbf{P}_0 = \mathbf{A};$

$\mathbf{P}_1 = \mathbf{B};$

$\mathbf{P}_2 = \mathbf{C};$

$\mathbf{P}_3 = \mathbf{D};$

$a = \text{round}(x \cdot m);$

$b = \text{round}(y);$

$id = a \cdot 2 + b;$

$t = (id \bmod 2) \wedge (\lfloor id/4 \rfloor \bmod 2);$

$l = \lfloor (id + 2)/4 \rfloor \bmod 2;$

$n = t + l \cdot 2;$

$\mathbf{V} = \mathbf{P}_n;$

**Algorithm 5:** This algorithm transforms tessellation coordinates into the vertex of side of shadow volume. Vertices **A, B, C, D** are computed using Equation 2.

fragments into depth of 1.0f, so they would fail the depth test, otherwise we observed self-shadowing artifacts. Bypassing early depth test in rasterization due to assigning depth values in fragment shader causes significant performance loss over two-pass method. This method served as a basis for silhouette-based approach.

For caps generation in silhouette-based method, we used gemetry shader and multiplicity calculation, using which we calculated triangle’s orientation towards light source via reference edge. It was also necessary for keeping discarding calculations consistent throughout the rendering process of shadow volumes.

Because tessellation factors are limited, at the time of writing, to 64, there is also a limit of maximum multiplicity per edge that this algorithm is able to process. According to equation to calculate tessellation factor  $Multiplicity \cdot 2 - 1$ , maximum multiplicity of an edge is 32, which should be more than enough for majority of models. But for example well-known Power Plant model (12M triangles) has some edges, which have multiplicity of 128. In that case, they would have to be splitted into more edges.

### 3 EXPERIMENTS

We compared our methods against already available shadow volumes implementations on modern hardware - robust geometry shader implementation and standard shadow mapping, using which we also tried to evaluate performance against Sintorn’s AFSM [Sintorn et al., 2008]. We also tested two-pass per-triangle method against similar geometry shader implementation. For shadow volumes approaches, z-fail was used; shadow map resolution was set to 8k x 8k texels.

Testing platform had following configuration: Intel Xeon E3-1230V3, 3.3 GHz; 16GiB DDR3; GPUs: AMD Radeon R9 280X 3 GiB GDDR5, nVidia

Spheres10x10 Triangles	R280				G680			
	TS		GS		TS		GS	
32400	984	<b>995</b>	490	484	739	<b>825</b>	542	540
67600	921	<b>963</b>	488	487	624	<b>667</b>	494	513
102400	615	<b>729</b>	484	479	491	<b>555</b>	372	402
360000	203	233	270	<b>272</b>	218	<b>228</b>	131	135
1081600	72	88	104	<b>110</b>	82	<b>94</b>	46	49
1440000	56	72	84	<b>91</b>	67	<b>81</b>	36	39
1960000	34	41	59	<b>62</b>	49	<b>58</b>	26	28

Table 1: Performance of two determinism methods measured in FPS on a scene with 10x10 spheres at different triangle count.

GeForce GTX 680 2GiB GDDR5; Windows 7 x64; driver version: 13.12 (AMD), 334.89 (nVidia).

### 3.1 Testing Scenes

We created a camera fly-through in two testing scenes, each having one point light source.

- Sphere scene: synthetic scene containing adjustable number of spheres (typically 100) with configurable amount of detailness. Fly-through has 16 seconds.
- Crytek Sponza: popular model used to evaluate computer graphics algorithms. 262 267 triangles, 40 seconds.

### 3.2 Results

Majority of our tests was performed on a sphere scene with adjustable amount of geometry. First, we made a flythrough in a scene containing 100 spheres with different amount of triangles per scene, the results can be seen in Table 1 and graph in Fig. 5.

On GTX680, tessellation using reference edge is the fastest, no matter the number of triangles, although the performance gaps gets smaller with increasing number of triangles in scene. R9 280X showed different results, tessellation was more than 2x faster when the scene contained only 32K triangles but at approximately 300K, geometry shader method took lead.

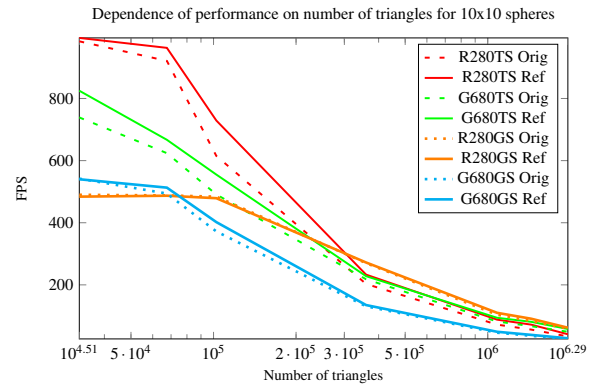


Figure 5: Dependence of performance (FPS) on number of triangles on a scene with 10x10 spheres using original and new deterministic method.

Spheres 1M Objects	R280				G680			
	TS		GS		TS		GS	
1	73	92	111	<b>120</b>	106	<b>134</b>	55	60
4	74	94	113	<b>121</b>	101	<b>126</b>	53	58
25	64	76	97	<b>101</b>	76	<b>88</b>	46	50
64	68	76	<b>90</b>	89	61	<b>66</b>	40	43
100	64	70	<b>84</b>	82	58	<b>62</b>	39	42
240	58	55	<b>70</b>	64	<b>50</b>	49	35	36
399	53	48	<b>61</b>	54	<b>36</b>	36	27	28
625	43	38	<b>53</b>	46	<b>29</b>	27	22	22
851	40	44	46	<b>50</b>	24	<b>25</b>	19	20
1250	35	<b>37</b>	28	31	<b>19</b>	19	16	16
2500	<b>23</b>	19	15.1	15.4	<b>12</b>	11	10.8	10.1
3116	21.2	<b>21.5</b>	12.8	12.5	11.1	<b>11.2</b>	9.1	9.2
3920	<b>15.7</b>	14	10.1	10.12	<b>9.1</b>	8.7	7.7	7.5
5100	<b>14.8</b>	14.2	7.8	7.75	<b>8.2</b>	8.2	6.7	6.8
15600	<b>7.45</b>	6.45	3.07	3.14	<b>10.5</b>	9.1	3.6	3.6

Table 2: Dependence on number of objects for spheres scene with 1M triangles. Bold values represent the fastest algorithm/implementation for respective number of objects, per GPU.

We further extended this test to performance dependency on number of objects in a scene while maintaining constant amount of geometry. This measurement was carried out on Sphere scene, having 1 million triangles (with deviation max 2%) in every case. No hardware instancing was used, every object was drawn via separate draw call. Results can be seen in Table 2 and graph in Figure 6.

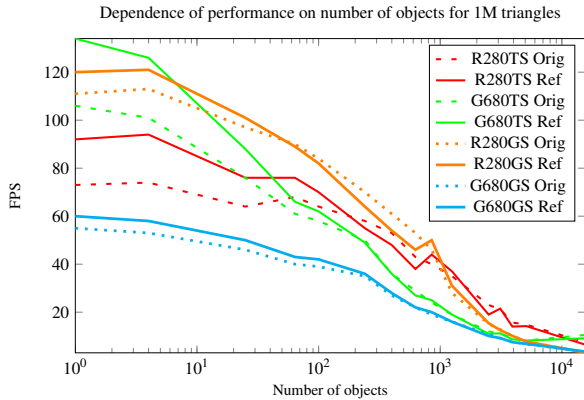


Figure 6: Dependence on number of objects for spheres scene with 1M triangles.

Contrary to previous measurements, tessellation was faster on R9 280X, starting from  $10^3$  objects, although reference edge was faster only in 40% cases. Moreover, as can be seen in Fig. 6, there is a slight increase in FPS in both geometry shader and tessellation implementations at about 1000 objects on Radeon. On GTX680, tessellation method was faster in every case; eference edge provided increased performance only in a half of measurements, but in all other cases the difference was only 1-3 FPS.

Sintorn in his AFSM paper Sintorn et al. [2008] stated that his per-pixel precise shadow maps are 3-times slower than standard 8Kx8K shadow mapping. In order to evaluate our algorithm against AFSM, we

Spheres 10x10 Triangles	R280		G680	
	TS	SM	TS	SM
32400	<b>995</b>	252	<b>825</b>	245
67600	<b>963</b>	250	<b>667</b>	237
102400	<b>729</b>	244	<b>555</b>	225
360000	<b>233</b>	219	<b>228</b>	190
1081600	88	<b>168</b>	94	<b>135</b>
1440000	72	<b>155</b>	81	<b>115</b>
1960000	41	<b>120</b>	58	<b>103</b>

Table 3: Shadow Mapping vs Tessellation Silhouettes, 10x10 sphere scene, FPS

conducted a measurement against shadow mapping having resolution mentioned above, results of which are in table 3 and graph 7.

Dependence of performance on number of triangles for Shadow Mapping and Tessellation Silhouettes

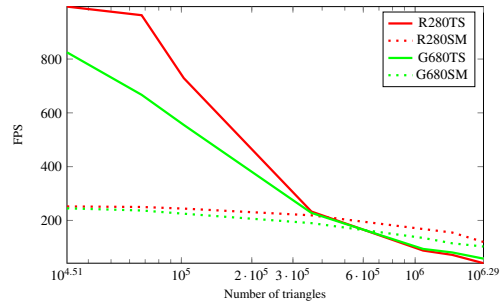


Figure 7: Shadow Mapping vs Tessellation Silhouettes on a scene with 10x10 spheres, measured in frames per second.

Not only we managed to outperform shadow mapping with triangle count up to  $\sim 400K$  triangles, but at almost 2M triangles our method was on par or faster than AFSM - R9 280X dropped to 34% of SM performance whereas GTX680 was only 44% slower than 8K shadow mapping.

We also compared silhouette methods with two-pass per-triangle tessellation implementation and 8K shadow mapping (only on sphere scene, our framework does not support omnidirectional shadow mapping) on Crytek Sponza scene, results in table 4 and graph 8.

One can observe that per triangle tessellation method is even faster than than both geometry shader methods running on Sponza scene. It is also worth noting that per-triangle geometry-shader-based method provides more performance on this scene than silhouette-based approach. On GTX680, the difference between silhouette and per-triangle tessellation method is 122%, whereas on R9 280X card it is only faster by 27%.

With increased amount of geometry in our synthetic test scene, the situation turns around in favor to silhouette methods. Also performance difference between shadow mapping and tessellation on Radeon drops under 1/3 ratio, but GeForce is still able to maintain 43% of SM performance.

## 4 CONCLUSIONS

We have developed new methods for computing shadow volume silhouettes using tessellation shaders.



Method	R280		G680	
	Spheres	Sponza	Spheres	Sponza
TS Triangle	5.8	102	7.9	83
TS Silhouette	23.7	130	32	185
GS Triangle	3.1	51	4.9	73
GS Silhouette	34	49	14.8	62
SM	93	0	74	0

Table 4: Overall comparison of GS, TS methods and classic 8K shadow mapping on testing scenes - Sponza, and Spheres with 4M triangles. Shadow mapping was not evaluated on Sponza scene (zeros).

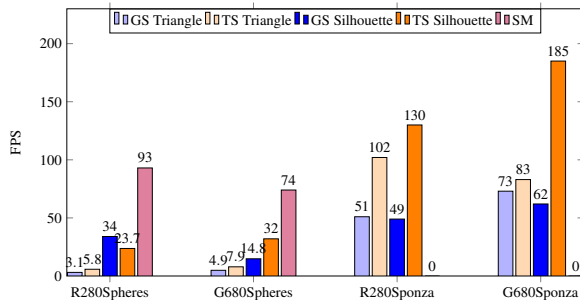


Figure 8: Overall comparison of methods on testing scenes - Sponza and Spheres with 4M triangles.

Our two-pass per-triangle tessellation method is, in some cases, faster than silhouette algorithm implemented in geometry shader, but loses performance as geometry amount in the scene grows. Compared to geometry shader per-triangle implementation, it was faster in every measurement.

The silhouette method is more efficient, and as we have proven in our measurements, mostly in scenes with higher amount of geometry. GeForce GTX680 benefited mostly from this algorithm, being faster than geometry shader silhouette method. As for Radeon R9 280X, geometry shader method is more suitable. Tessellation method on Radeon proved to be faster in Sponza scene, but our synthetic tests on sphere scene showed that it's performance is dominant only up to ~300K of triangles when having multiple objects in the scene, or only up to 15K triangles when only a single detailed object was drawn. In less detailed scenes it was able to outperform nVidia-based card, but only up to aforementioned 300K triangles.

Our robust algorithm was sped up by using a novel method of multiplicity computation, which was able to provide up to 31% performance gain in tessellation method (13.5% in average), maximum speedup in geometry shader was 10.7% with average of 3.4%.

In comparison to standard SM and Sintorn's Alias-Free Shadow Maps (AFSM), our tessellation method provides better performance than 8K shadow maps up to ~400K triangles and then fall to 43% performance of shadow mapping at 4M triangles on GeForce, 34% on Radeon, which is on par or better than AFSM (it's 3-times slower than 8K SM) and is also simpler to implement.

In the future, we would like to see an arbitrary  $\pm$  stencil operation in hardware, configurable in shaders, which would allow us to increase the speed of our method even more, due to a lower number of triangles being drawn. We also want to evaluate more hardware platforms and explore GPGPU potential in the field of shadow volumes calculation.

## ACKNOWLEDGEMENTS

The work has been made possible thanks to the co-funding by the IT4Innovations Centre of Excellence, Ministry of Education, Youth and Sports, Czech Republic, MŠMT, ED1.1.00/02.0070, V3C - Visual Computing Competence Center, Technology Agency of the Czech Republic, TAČR, TE01020415V3C, and RODOS - Transport systems development centre, Technology Agency of the Czech Republic, TAČR, TE01020155.

## REFERENCES

- Brabec, S. and Seidel, H.-P. (2003). Shadow volumes on programmable graphics hardware. *Computer Graphics Forum (Eurographics)*, 2003:433–440.
- Crow, F. C. (1977). Shadow algorithms for computer graphics. In *Proceedings of the 4th annual conference on Computer graphics and interactive techniques*, SIGGRAPH '77, pages 242–248, New York, NY, USA. ACM.
- Donnelly, W. and Lauritzen, A. (2006). Variance shadow maps. In *Proceedings of the 2006 Symposium on Interactive 3D Graphics and Games*, I3D '06, pages 161–165. ACM.
- Everitt, C. and Kilgard, M. J. (2002). Practical and robust stenciled shadow volumes for hardware-accelerated rendering.
- Heidmann, T. (1991). Real shadow real time. pages 28–31. IRIS Universe.
- Kim, B., Kim, K., and Turk, G. (2008). A shadow-volume algorithm for opaque and transparent nonmanifold casters. *J. Graphics Tools*, 13(3):1–14.
- McGuire, M., Hughes, J. F., Egan, K., Kilgard, M., and Everitt, C. (2003). Fast, practical and robust shadows. Technical report, NVIDIA Corporation, Austin, TX.
- Pečiva, J., Starka, T., Milet, T., Kobrtek, J., and Zemčík, P. (2013). Robust silhouette shadow volumes on contemporary hardware. In *Conference Proceedings of GraphiCon'2013*, pages 56–59. GraphiCon Scientific Society.
- Sintorn, E., Eisemann, E., and Assarsson, U. (2008). Sample based visibility for soft shadows using alias-free shadow maps. *Computer Graphics Forum (Proceedings of the Eurographics Symposium on Rendering 2008)*, 27(4):1285–1292.
- Sintorn, E., Olsson, O., and Assarsson, U. (2011). An efficient alias-free shadow algorithm for opaque and transparent objects using per-triangle shadow volumes. In *ACM SIGGRAPH Asia 2011*, SIGGRAPH Asia 2011.
- Stich, M., Wächter, C., and Keller, A. (2007). Efficient and robust shadow volumes using hierarchical occlusion culling and geometry shaders. In Nguyen, H., editor, *GPU Gems 3*, pages 239–256. Addison Wesley Professional.
- Williams, L. (1978). Casting curved shadows on curved surfaces. *SIGGRAPH Comput. Graph.*, 12(3):270–274.